Journal of Luminescence 159 (2015) 105–109

Contents lists available at ScienceDirect

Journal of Luminescence

journal homepage: www.elsevier.com/locate/jlumin

Luminescence enhancement of PPO/PVT scintillators by CeF_3 nanoparticles

Sunil Sahi, Wei Chen *, Ke Jiang

Department of Physics and the SAVANT Center, University of Texas at Arlington, Arlington, TX 76019-0059, USA

ARTICLE INFO

Article history:
Received 6 May 2014
Received in revised form
22 September 2014
Accepted 4 November 2014
Available online 13 November 2014

Keywords:
Cerium fluoride
PPO
X-ray Excited Optical Luminescence
Energy transfer
Nanocomposites
Photoluminescence

ABSTRACT

Oleic acid coated cerium fluoride (CeF_3) nanoparticles were synthesized by a wet chemistry method. The average size of the nanoparticles is 12 nm, and the nanoparticles are dispersible in polyvinyl toluene (PVT) monomer due to the oleic acid coating. Different amounts of as-synthesized CeF_3 nanoparticles are then loaded into PVT matrix with 0.5 wt% 2,5-diphenyloxazole (PPO) by bulk polymerization. The luminescence of PPO/PVT is enhanced by CeF_3 nanoparticles to 3 and 2.5 times under UV and X-ray excitation, respectively. This enhancement is due to the energy transfer from CeF_3 to PPO, the increase of the stopping power by doping CeF_3 nanoparticles into PPO/PVT and the escape of charges from CeF_3 nanoparticles.

1. Introduction

The development of high-performance scintillating materials is essential for precision calorimetry in high energy physics [1], medical imaging [2] and industries [3]. The most frequently considered characteristics of scintillators are efficiency of energy conversion, stopping power, luminescence decay time, spatial resolution, and physical and chemical stability [4]. Currently applied inorganic crystalline scintillators are not only limited by their high cost and scalability issues, but also limited by other intrinsic drawbacks. For example, high purity germanium must be operated at liquid nitrogen temperature, while sodium iodide crystal is highly hygroscopic. On the other hand, plastic scintillators based on polymeric materials are cheap and easy to manufacture, but have low light yield and low density [5]. Also, it has been reported that the plastic scintillator loses its optical and mechanical properties as the radiation doses increase [6]. These limit the application of plastic scintillator for high energy gamma-ray detection. Hence, the drawbacks of conventional inorganic and organic scintillators necessitate new generation of scintillators which could combine high performance of inorganic scintillating materials with scalability of polymer materials. One practical approach is to make nanocomposite materials which consist of high density and high-performance scintillating nanoparticles embedded in a polymer matrix maintaining the transparency of the matrix.

Transparent nanocomposites can be obtained by index matching of the filler and the matrix. However, literature reported that sufficiently small size of the filler could lead to minimized optical scattering even with a large mismatch of refractive index [7]. Based on this, many approaches have been taken to make composite materials consisting of high Z nanomaterials embedded in different matrix (polymer or glass) for scintillator application. The main goal is to enhance the luminescence of nanocomposites by incorporation of high Z material, so that it can be used for gamma ray spectroscopy. Early development of composite scintillators used a grinding method, but resulting in materials that were not transparent [8]. Kang et al. used index matching of nanoparticles and the polymer matrix to make nanocomposites with high transparency [9]. Polymer composite film with BiI_3 and conjugated polymer reported by Zhong et al. exhibits photoluminescence quenching due to the charge transfer from the polymer matrix to BiI_3 [10]. Feller et al. used oleic acid as both a ligand and a matrix to achieve high nanoparticle loading while keeping the transparency up to 70% [11]. Cai et al. used non-fluorescent Gd_2O_3 nanocrystals dispersed in PVT matrix and reported enhanced luminescence due to fluorescence resonance energy transfer (FRET) from the matrix to the fluor [12]. Also, nanoporous glass was used as a matrix for CdSe/ZnS core/shell quantum dots by Letant and Wang, which shows better energy resolution of 59-keV americium-241 than that of NaI single crystal [13]. Yao et al. loaded LaF_3:Ce nanoparticles in to ORMOSILs for scintillator application [14]. It has also been reported that the energy transfer based nanocomposite material could be a potential material for the radiation detection [15,16]. In this work we have used nanoparticles of known heavy scintillator materials along with known scintillating organic fluor as fillers and polyvinyl toluene (PVT) as

* Corresponding author.

http://dx.doi.org/10.1016/j.jlumin.2014.11.004
0022-2313/

a matrix. The nanocomposites show enhancement in the luminescence due to FRET energy transfer from the nanoparticle to the organic fluor.

In the last decade rare earth fluoride nanoparticles were extensively studied for various applications [17–21]. Among the rare earth fluorides, cerium fluoride (CeF_3) nanoparticles have been of particular interest due to the Ce^{3+} emission. CeF_3 nanoparticles were synthesized using different techniques from hydrothermal [22], solvothermal [23], extraction method [24], microwave [25], sonication assisted method [26], reverse micelles route [27], microemulsion [28,29] to wet chemistry [19]. First identified as a scintillator in 1989, CeF_3 is known as an appealing scintillating material due to its high density and short decay time [30]. However, the emission of CeF_3 lies within UV range, which is not suitable for direct detection by photomultiplier tube and photodiode. Therefore, a wavelength shifter is needed to transfer the emission energy from CeF_3 to higher wavelength. For this purpose, 2,5-diphenyloxazole (PPO) is selected due to its appropriate luminescent properties. Furthermore, PPO has already been widely used as a fluor in plastic scintillators. Here, we have chosen PVT as an organic polymer matrix that has been widely used as a base for plastic scintillator due to its ease of fabrication and low cost. We have synthesized CeF_3 nanoparticles coated with oleic acid and embedded these nanoparticles into the polymer matrix along with PPO to make nanocomposite scintillators. Enhancement in the luminescence of PPO has been observed under ultraviolet (UV) and X-ray excitations.

2. Experimental

2.1. Chemicals

Cerium (III) nitrate hexahydrate (99.9% trace metal basis), sodium fluoride (ACS reagent, ≥99%), 2,5-diphenyloxazole (99%), and benzoyl peroxide (97%) were purchased from Sigma-Aldrich. Oleic acid (90%) and 4-methylstyrene (98+%, stab. with 0.1% 3,5-di-tert-butylcatechol) were purchased from Alfa-Aesar.

2.2. Synthesis of cerium fluoride nanoparticles

In this work, CeF_3 nanoparticles were synthesized via a precipitation reaction. Briefly, 30 mmol sodium fluoride (NaF) was dissolved into 80 mL of D.I water and mixed with 80 mL of ethanol solution containing 1.5 mL oleic acid. The mixture was heated to 80 °C under vigorous stirring with purging of argon gas. 10 mmol of $Ce(NO_3)_3 \cdot 6H_2O$ was then dissolved into 60 mL of DI water and added into the above mixture dropwise. The reaction was kept as 80 °C for 4 h and then allowed to cool in the air. The precipitates were collected by centrifugation and washing with ethanol for three times and then dried at 50 °C for 12 h under vacuum.

2.3. Preparation of CeF_3/PPO/PVT nanocomposites

After removal of the polymerization inhibitor from PVT monomers using a silica column, benzoyl peroxide (as the free radical initiator) (0.1 wt%) and PPO (0.5 wt%) were dissolved in PVT monomer solution and subjected to ultrasonication for 20 min. Then, different concentrations (wt%) of CeF_3 nanoparticles were added into the above mixture and further sonicated for 45 min. During the first 45 min of the incubation process at 75 °C, the CeF_3 nanoparticle-contained PVT monomer solution was agitated with vortex mixture for several times to ensure a good dispersion of CeF_3 nanoparticles in the monomer. After these treatments, the polymerization of PVT monomers has been sufficiently initiated so that the enhanced viscosity would prevent CeF_3 nanoparticles from aggregation. The composite was then allowed to be incubated at 75 °C for 90 h and then cooled down to room temperature. Free-standing CeF_3/PPO/PVT composites were then obtained after removing the glass container.

2.4. Instrumentation

The HRTEM images of the particles were obtained using a JEOL JEM-2100 electron microscope with accelerating voltage of 200 kV. Optical absorption was recorded with a SHIMADZU UV-2450 spectrophotometer. Photoluminescence emission (PL) and excitation (PLE) were taken on a SHIMADZU RF-5301 PC Spectrofluorometer. X-ray Excited Optical Luminescence (XEOL) was measured in a light-proof X-ray cabinet equipped with optic fiber connection to an outside detector. X-ray irradiation (90 kV_p and 5 mA) was performed using a Faxitron RX-650 X-ray cabinet (Faxitron X-ray Corp., IL, USA). The luminescence spectra were recorded using a QE65000 spectrometer (Ocean Optics Inc., Dunedin, FL) connected to the X-ray chamber using a 600 μm core diameter, P600-2-UV–vis fiber optic (Ocean Optics Inc., Dunedin, FL). XRD were recorded using a Siemens Kristalloflex 810 D-500 X-ray diffractometer operating at 40 kV voltage and 30 mA current with a radiation beam of $\lambda = 1.5406$ Å.

3. Results and discussion

The XRD pattern is shown in Fig. 1, illustrating the hexagonal phase of crystalline CeF_3. Fig. 2(A) shows the TEM images of CeF_3 nanoparticles. The histogram shown in Fig. 2(B) indicates that the average size of as-prepared CeF_3 nanoparticles is about 12 nm. The presence of oleic acid on the nanoparticle surfaces not only significantly reduces the size of CeF_3 nanoparticles, but also enables the uniform dispersion of the nanoparticles into the polymer matrix. It was utilized to confine the growth of CeF_3 crystals so that small particle sizes can be achieved for minimizing light scattering.

Fig. 3 shows photoluminescence emission (PL) and excitation (PLE) of CeF_3 nanoparticles along with the absorption spectrum of PPO/PVT. CeF_3 nanoparticle has an excitation peak at 290 nm and an emission peak at 330 nm. CeF_3 exhibits several excitation bands, and the low energy one is centered about 250 nm when saturation effect is discarded. The emission of CeF_3 crystals is usually centered at 305 nm which is attributed to the 5d–4f transition of the Ce^{3+} ion [31,32]. The emission at 330 nm in our CeF_3 nanoparticles is mainly from surface states as pointed by Dujardin et al. [33].

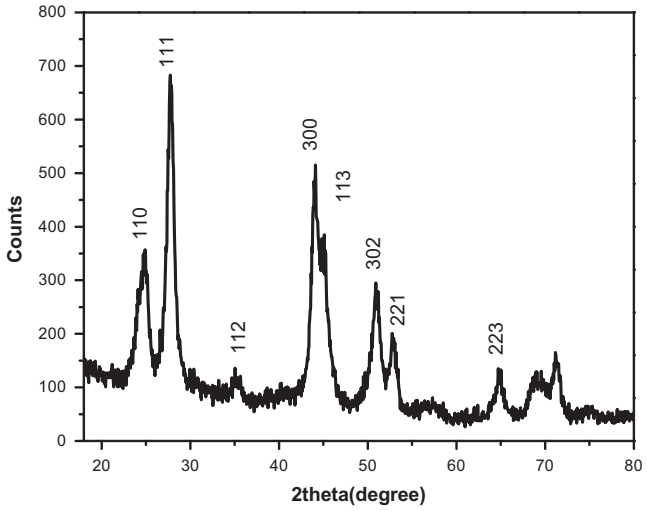

Fig. 1. XRD pattern of the as synthesized CeF_3 nanoparticles.

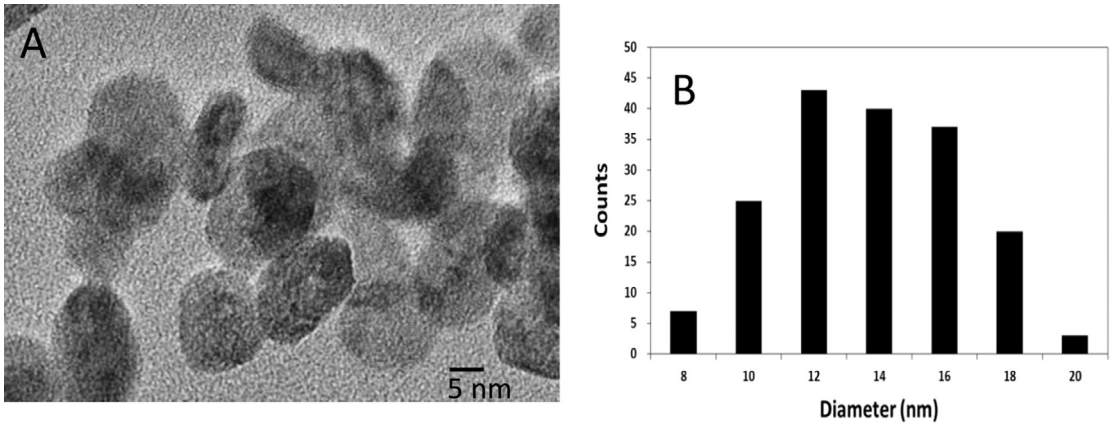

Fig. 2. (A) HR-TEM image and (B) size distribution of CeF_3 nanoparticles.

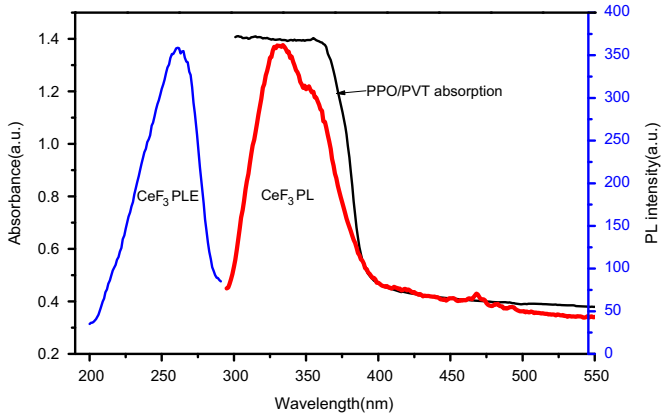

Fig. 3. Photoluminescence emission (PL) and excitation (PLE) of as synthesized CeF_3 nanoparticles and absorption spectrum of PPO/PVT.

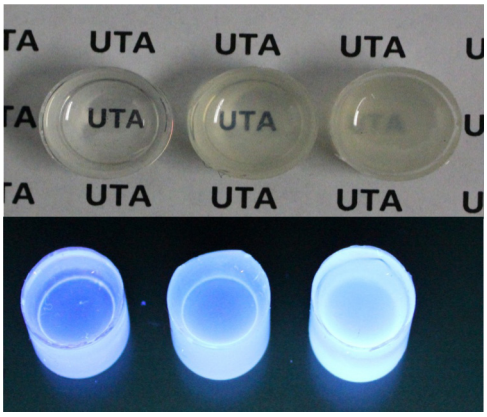

Fig. 4. Picture of CeF_3 loaded (0 wt%, 5 wt% and 10 wt% from left to right) PPO/PVT composite under normal light (top panel) and under UV light (bottom panel).

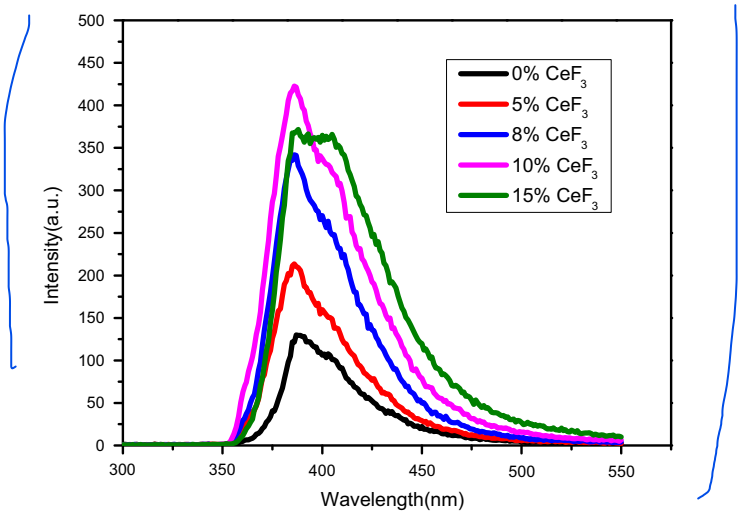

Fig. 5. Photoluminescence of PPO/PVT with different loading concentrations of CeF_3 nanoparticles.

The emission in CeF_3 nanoparticle overlaps with the absorption of PPO/PVT and fulfill the condition for FRET. It is expected that the energy can be transferred from CeF_3 nanoparticles to PPO/PVT due to this FRET overlapping. The lifetime of ~330 nm emission of CeF_3 is ~30 ns [30,31], and that of PPO is 1.6 ns [34] as reported by various authors. These lifetimes also fulfill the criteria that the donor lifetime must be sufficiently longer than that of acceptor for FRET to occur. When being excited at 290 nm, PPO/PVT shows an emission band peaking at around 390 nm. To elucidate the enhancement effect of CeF_3 doping on the emission of PPO/PVT composites, different concentrations of CeF_3 nanoparticles are loaded into PVT matrix while the concentration of PPO was kept constant at 0.5 wt%. Nanocomposites loaded with CeF_3 nanoparticles exhibited brighter emissions under UV-light as compared to the unloaded sample, as can be seen in Fig. 4. The room temperature photoluminescence spectra of nanocomposites excited at 290 nm are shown in Fig. 5. It is clear that CeF_3 nanoparticles significantly enhanced the photoluminescence of PPO/PVT composites. This enhancement in the emission intensity of nanocomposites loaded with CeF_3 nanoparticles is due to the energy transfer from CeF_3 to PPO in PVT matrix as expected. Also, there is no shift in PPO emission position in the nanocomposites. In addition, the photoluminescence spectra of CeF_3/PPO/PVT composites do not show any emission from CeF_3 nanoparticles when being excited at 290 nm wavelength, which further supported the argument that the enhancement in photoluminescence is due to the FRET from CeF_3 nanoparticles to PPO/PVT composite.

The mechanism of energy transfer can be explained using the energy level diagram as shown in Fig. 6. Upon irradiation with UV or X-ray, excitons are generated on CeF_3 nanocrystals. Since the emission of CeF_3 overlaps perfectly with the absorption of PPO in PVT, excitions on the nanoparticles can transfer their energy to PPO in PVT matrix as long as the distance between nanoparticles and fluor molecules reaches the critical radius as required by FRET principles [35]. Once excitons transfer their energy to PPO, they would recombine to give luminescence. Enhancement in PL is more than 3 times for the CeF_3 loading concentration of 10 wt% and then decreases to about 2.8 times for 15 wt%. This decrease in PL with

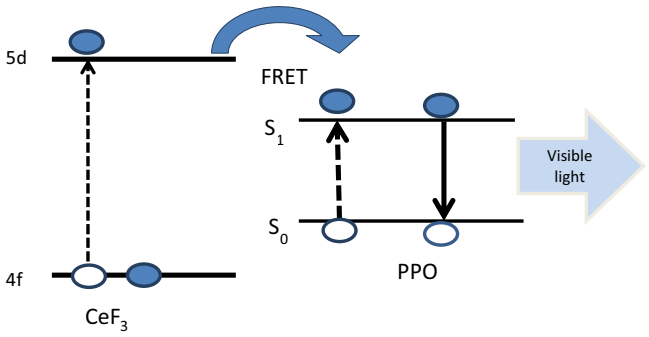

Fig. 6. Mechanism of fluorescence resonance energy transfer (FRET) from CeF_3 to PPO.

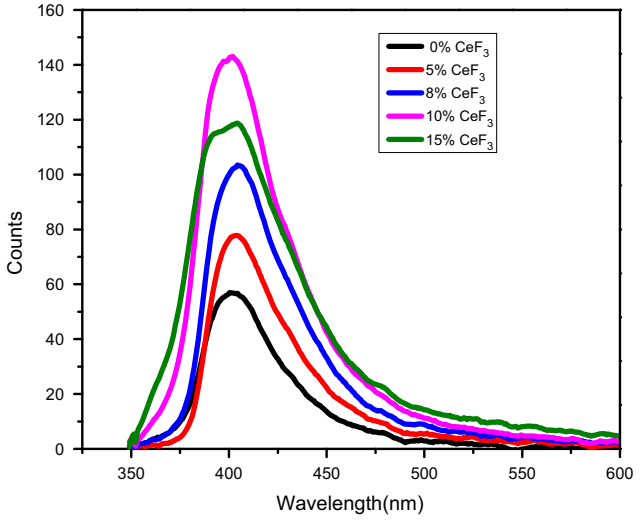

Fig. 7. XEOL of PPO/PVT with different loading concentrations of CeF_3 nanoparticles.

higher loading concentration might be due to the increased population of the non-radiative triplet state or the loss of transparency of the nanocomposites at higher nanoparticle loading concentrations. As shown in Fig. 4, the transparency of the nanocomposites decreases with increasing nanoparticle loading concentration.

Since the energy transfer mechanism is similar in case of both UV and X-ray excitations, we have used X-ray as an excitation source to provide further evidences of energy transfer in the nanocomposites. We have employed 90 kV_p X-ray as an excitation source to measure the X-ray Excited Optical Luminescence (XEOL) of the nanocomposites. Fig. 7 shows the XEOL of nanocomposites with different nanoparticle loading concentrations. Again, enhanced luminescence was observed for nanocomposites loaded with CeF_3 nanoparticles under X-ray excitation. This further strengthens the energy transfer evidence. Also no CeF_3 emission is seen under X-ray excitation, which is due to the strong absorption of PPO/PVT composite in the region of CeF_3 emission. In case of X-ray excitation, the peak is red shifted by 10 nm in all the nanocomposites and enhancement is 2.5 times for the loading concentration of 10 wt% compared to only PPO/PVT composite, as shown in Fig. 7. Again, at a higher nanoparticle loading concentration (15 wt%), the enhancement of XEOL decreased to 2.1 times as compared to the one without nanoparticle. Thus, energy transfer from CeF_3 nanoparticle to PPO/PVT is observed when the nanocomposites are excited by both UV and X-ray sources.

It should be pointed out that, in addition to energy transfer, the increase of the stopping power by doping CeF_3 nanoparticles into PPO/PVT and the escape of charges from CeF_3 nanoparticles also contribute to the luminescence enhancement. For the same reasons, we believe the quenching of CeF_3 emission is due to energy transfer, self-absorption, charge escape as well as the surface modification when doped into PPO/PVT. Energy transfer is a complex process and more studies are necessary to prove the energy transfer and mechanism. The fluorescence resonance energy transfer (FRET) process involves a pair of dissimilar fluorophores in close proximity, typically less than 10 nm apart. The shorter-wavelength fluorophore (donor) is directly excited with incident light, and then transfer's energy nonradiatively to the longer-wavelength fluorophore (acceptor), which then emits light. In this case, the excitation wavelength is chosen for maximum absorption by the donor, but the emitted light is characteristic of the acceptor. The magnitude of the FRET signal is extremely dependent on the separation between the fluorophores, and so can be used to monitor binding events and conformational changes. In the case of PPO/PVT by CeF_3, we believe the energy transfer is simply due to the absorption of the emission energy from CeF_3 nanoparticles by PPO/PVT organic scintillators. However, energy transfer is not the only reason for the luminescence enhancement or the quenching of CeF_3 luminescence. More studies are needed in order to understand the optical processes occurred in these materials.

4. Conclusion

CeF_3 nanoparticles were synthesized and their emission is at 330 nm which is mainly from surface states. Enhanced luminescence is observed in PPO/PVT scintillators when embedded with CeF_3 nanoparticles. Enhancement in the PL is more than 3 times for 10 wt% of CeF_3 loading whereas enhancement is 2.5 times when X-ray is used as excitation source for the same nanoparticles loading concentration. The luminescence enhancement in PPO/PVT by CeF_3 nanoparticles is attributed to the energy transfer, the increase of the stopping power by doping CeF_3 nanoparticles as well as the escape of charges from CeF_3 nanoparticles. The observations provide a new method to improve PPO/PVT organic scintillators for radiation detection.

Acknowledgment

We would like to acknowledge the support from the startup funds from UTA, the NSF (CBET-0736172) and DHS-DNDO ARI program (2011-DN-077-ARI053-02, 3, 4 &5).

References

[1] P. Lecoq, J. Lumin. 60–61 (1994) 948.
[2] C.W.E. van Eijk, Nucl. Instrum. Methods Phys. Res. Sect. A—Accel. Spectrom. Detect. Assoc. Equip. 509 (1–3) (2003) 17.
[3] C.L. Melcher, Industrial applications of scintillators, in: F. DeNotaristefani, P. Lecoq, M. Schneegans (Eds.), Heavy Scintillators for Scientific and Industrial Applications—Crystal 20001993, pp. 75–84.
[4] C.W.E. van Eijk, Nucl. Instrum. Methods Phys. Res. Sect. A—Accel. Spectrom. Detect. Assoc. Equip. 460 (1) (2001) 1.
[5] B.L. Rupert, et al., Europhys. Lett. 97 (2) (2012) 22002.
[6] H.M. Hamada, et al., Nucl. Instrum. Methods Phys. Res. Sect. A—Accel. Spectrom. Detect. Assoc. Equip. 422 (1–3) (1999) 148.
[7] E.A. McKigney, et al., Nucl. Instrum. Methods Phys. Res. Sect. A—Accel. Spectrom. Detect. Assoc. Equip. 579 (1) (2007) 15.
[8] V.G. Vasil'chenko, A.S. Solov'ev, Instrum. Exp. Tech. 46 (6) (2003) 758.
[9] Z. Kang, et al., J. Lumin. 131 (10) (2011) 2140.
[10] H. Zhong, et al., Nanotechnology 19 (2008) 50.
[11] R.K. Feller, et al., J. Mater. Chem. 21 (15) (2011) 5716.
[12] W. Cai, et al., J. Mater. Chem. C 1 (10) (2013) 1970.
[13] S.E. Letant, T.F. Wang, Nano Lett. 6 (12) (2006) 2877.
[14] M. Yao, et al., J. Appl. Phys. 113 (2013) 1.
[15] M. Hossu, et al., Appl. Phys. Lett. 100 (2012) 1.
[16] S. Sahi, W. Chen, Radiat. Meas. 59 (0) (2013) 139.
[17] Y. Liu, et al., J. Appl. Phys. 103 (6) (2008) 063105.

[18] Y. Liu, et al., Appl. Phys. Lett. 92 (2008) 4.
[19] Z. Sun, et al., J. Nanosci. Nanotechnol. 9 (11) (2009) 6283.
[20] Y. Liu, Q. Ju, X. Chen, Rev. Nanosci. Nanotechnol. 1 (3) (2012) 163.
[21] L.G. Jacobsohn, et al., J. Nanomater. 2011 (2011) (Article ID: 523638).
[22] C. Li, et al., J. Phys. Chem. C 112 (39) (2008) 15602.
[23] X. Qu, et al., J. Solid State Chem. 184 (2) (2011) 246.
[24] L. Wang, et al., Mater. Res. Bull. 43 (8–9) (2008) 2220.
[25] L. Ma, et al., Mater. Lett. 64 (14) (2010) 1559.
[26] D. Arun Kumar, et al., Solid State Sci. 14 (5) (2012) 626.
[27] H. Zhang, et al., J. Colloid Interface Sci. 302 (2) (2006) 509.
[28] Q. Sunqing, D. Junxiu, C. Guoxu, Wear 230 (1) (1999) 35.
[29] S. Qiu, J. Dong, G. Chen, Powder Technol. 113 (1–2) (2000) 9.
[30] W.W. Moses, S.E. Derenzo, IEEE Trans. Nucl. Sci. 36 (1) (1989) 173.
[31] W.W. Moses, et al., J. Lumin. 59 (1–2) (1994) 89.
[32] C.W.E. vanEijk, Nucl. Instrum. Methods Phys. Res. Sect. A—Accel. Spectrom. Detect. Assoc. Equip. 392 (1–3) (1997) 285.
[33] C. Dujardin, et al., IEEE Trans. Nucl. Sci. 57 (3) (2010) 1348.
[34] R. Luchowski, Chem. Phys. Lett. 501 (4–6) (2011) 572.
[35] M.-C. Chirio-Lebrun, M. Prats, Biochem. Educ. 26 (4) (1998) 320.